

Published in final edited form as:

Biomaterials. 2014 August ; 35(26): 7647–7653. doi:10.1016/j.biomaterials.2014.05.045.

Turning a Water And Oil Insoluble Cisplatin Derivative into a Nanoparticle Formulation for Cancer Therapy

Shutao Guo, Yuhua Wang, Lei Miao, Zhenghong Xu, C. Michael Lin, and Leaf Huang*

Division of Molecular Pharmaceutics and Center for Nanotechnology in Drug Delivery, Eshelman School of Pharmacy, University of North Carolina at Chapel Hill, Chapel Hill, NC 27599

Abstract

The formulation of water insoluble organic compounds into nanoparticles has become a widely established method for enhancing the delivery and efficacy of cancer therapeutics. Therefore, a comparable approach when applied to water insoluble inorganic compounds should also promote similar advantages. Herein, we have successfully formulated insoluble iodinated cisplatin (CDDP-I) into a LPI NPs (lipid-coated iodinated CDDP nanoparticles). Two separate microemulsions were combined, each containing a precursor for the synthesis of CDDP-I. The resulting CDDP-I precipitate was then coated with an anionic lipid and dispersed in water with the help of an additional lipid. This method allows us to effectively encapsulate CDDP-I and was able to achieve a considerable drug loading of 82 wt%. Administered LPI NPs demonstrated high level accumulation in tumor tissues and exhibited an anti-cancer activity comparable to free CDDP in two melanoma xenograft models without inducing nephrotoxicity. The benefits offered through this delivery formulation are not unique to CDDP-I, as this versatile platform may be extended to the formulation of other inorganic compounds that are both water and oil insoluble into nanoparticles for superior anticancer efficacy.

Keywords

Cisplatin; Nanoparticle; Inorganic drug; Liposome

1. Introduction

The application of cisplatin (CDDP), an established anticancer drug, is hampered by severe side effects such as neuro- and nephro-toxicity, which limit the maximum tolerated dose (MTD) of cisplatin [1, 2]. To overcome these shortcomings, derivatives incorporating more stable leaving groups, such as carboplatin and oxaliplatin, have been synthesized to reduce side effects. Yet, such modifications inadvertently diminish the efficacy [3, 4]. Another

© 2014 Elsevier Ltd. All rights reserved.

*Address correspondence to: Dr. Leaf Huang, Division of Molecular Pharmaceutics and Center for Nanotechnology in Drug Delivery, Eshelman School of Pharmacy, University of North Carolina, Chapel Hill, NC 27599, USA. leafh@unc.edu, Tel.: +1 919 843 0736; fax: +1 919 966 0197.

Publisher's Disclaimer: This is a PDF file of an unedited manuscript that has been accepted for publication. As a service to our customers we are providing this early version of the manuscript. The manuscript will undergo copyediting, typesetting, and review of the resulting proof before it is published in its final citable form. Please note that during the production process errors may be discovered which could affect the content, and all legal disclaimers that apply to the journal pertain.

potential strategy has been to alter the halide leaving groups [5]. After this alteration, bromide retains activity and exhibits potent anti-tumor efficacy while iodinated CDDP (CDDP-I) is ineffective, probably due to its insolubility [5, 6].

Nanoparticulate formulations have been developed to enhance the accumulation of CDDP in tumors through the enhanced permeability and retention (EPR) effect while reducing side effects through a restricted drug distribution [7, 8]. Unlike paclitaxel, a water insoluble but oil soluble anti-tumor drug, CDDP-I, is insoluble in any organic solvent and cannot be formulated into nanoparticles (NP) or liposomes. However, formation of CDDP-I nanocrystals may be achieved using “top-down” technology, which involves breakdown of large drug particles through a milling process [9–11]. Most nanocrystal formulations are administered orally even though nanocrystals dissociate quickly in the blood stream. Taking advantage of this property, we aim to develop a CDDP-I formulation for intravenous administration.

In previous work, CDDP was used to construct LPC NPs [12] in a microemulsion reactor using the CDDP precursor and potassium chloride (KCl). Drug loading efficiency for this NP formulation was high (80 ± 5 wt%). CDDP-I was synthesized through a reaction between potassium iodine (KI) and the CDDP precursor in a microemulsion to make cores which were dispersed in water (Scheme 1). Dioleoyl phosphatidic acid (DOPA), an anionic lipid, was used to stabilize the CDDP-I cores, which were further dispersed using an outer leaflet lipid layer to obtain LPI NPs (lipid-coated iodinated CDDP nanoparticles). Cell toxicities of LPI NPs and release of CDDP-I from LPI NPs were evaluated then. Tumor accumulation, anti-tumor effect and safety of LPI NPs were also investigated.

2. Materials and methods

2.1. Materials

Lipids were purchased from Avanti Polar Lipids (Alabaster, AL). Dulbecco's Modified Eagle Medium (DMEM), L-glutamine, penicillin G sodium, streptomycin and fetal calf serum were purchased from Gibco®. DSPE-PEG-AA was synthesized in our laboratory as previously reported [13]. 1-Hexanol was purchased from Alfa Aesar. Igepal®CO-520, triton™ X-100, cyclohexane, CDDP and silver nitrate were obtained from Sigma-Aldrich (St Louis, MO) without further purification. Pluronic P85 was purchased from BASF Corporation (North Mount Olive, NJ).

2.2. Cell Lines

A375M and 1205Lu cells were cultured in DMEM medium supplemented with 10% heat-inactivated fetal bovine serum (FBS), 20 mM of L-glutamine, 100 U/mL of penicillin G sodium, and 100 mg/mL of streptomycin at 37 °C in an atmosphere of 5% CO₂ and 95% air.

2.3. Synthesis of cis-[Pt(NH₃)₂(H₂O)₂](NO₃)₂ Precursor

Briefly, AgNO₃ (66.2 mg, 0.39 mmol) was added to a suspension of CDDP (60 mg, 0.20 mmol) in 1.0 mL water. The mixture was heated at 60 °C for 3 h and then stirred overnight in a flask protected from light with aluminum foil. The mixture was then centrifuged at

16,000 rpm for 15 min to remove the AgCl precipitate. The solution was filtered using a 0.2 μm syringe filter. The concentration of cis-[Pt(NH₃)₂(H₂O)₂](NO₃)₂ was measured using ICP-MS and adjusted to 200 mM.

2.4. Preparation of LPI NPs

The synthesis of LPI NPs is described in Scheme 1. First, 100 μL of 200 mM cis-[Pt(NH₃)₂(H₂O)₂](NO₃)₂ was dispersed in a solution composed of a mixture of cyclohexane/Igepal®CO-520 (71:29, V:V) and cyclohexane/triton-X100/hexanol (75:15:10, V:V:V) to form a well-dispersed, water-in-oil reverse micro-emulsion. Another emulsion containing KCl was prepared by adding 100 μL of 800 mM KI in water into a separate 8.0 mL oil phase. One hundred μL of DOPA (20 mM) was added to the CDDP precursor phase and the mixture was stirred. Twenty min later, the two emulsions were mixed and the reaction proceeded for another 30 min. Following the reaction, 16.0 mL of ethanol was added to break the micro-emulsion and the mixture was centrifuged at 12,000 g for at least 15 min to remove the cyclohexane and surfactants. After being extensively washed with ethanol 2–3 times, the pellets were re-dispersed in 3.0 mL of chloroform and stored in a glass vial for further modification.

To prepare the final NPs, 1.0 mL of CDDP-I core, 100 μL of 20 mM 1,2-dioleoyl-3-trimethylammonium-propane (chloride salt) (DOTAP)/cholesterol (molar ratio 1:1) and 50 μL of 10 mM DSPE-PEG-2000 or DSPE-PEG-AA were combined. After evaporating the chloroform, the residual lipids were dispersed in 1.0 mL of d-H₂O.

2.5. Characterization of NPs

The zeta potential and particle size of LPI NPs were determined using a Malvern ZetaSizer Nano series (Westborough, MA). TEM images were acquired using a JEOL 100CX II TEM (JEOL, Japan). The LPI NPs was negatively stained with 2% uranyl acetate. The drug-loading capacity and platinum content were measured using inductively coupled plasma mass spectrometry (ICP-MS).

2.6. Cell Toxicity Assay

A375M and 1205Lu cells were seeded in 96-well plates at a density of 2000 cells/well and incubated in a 10:1 ratio of DMEM and FBS containing 100 U/mL penicillin, and 100 mg/mL streptomycin for 20 h. The medium was then removed and replaced by Opti-MEM containing CDDP or LPI NPs. Forty-eight hours later, a CellTiter 96 Aqueous One Solution Cell Proliferation Assay kit (Promega, Madison, WI) containing the tetrazolium compound MTS was used to assay cell viability according to the manufacturer's protocols. IC₅₀ values were calculated using Graphpad Prism 5 (Graphpad Software Inc.).

2.7. Cellular Uptake

A375M cells were seeded in 24-well plates at a density of 3×10^4 cells per well and incubated for 20 h in 10% FBS of DMEM containing 100 U/mL penicillin, and 100 mg/mL streptomycin. The medium was then removed and replaced by 100 μM of Opti-MEM containing CDDP or LPI NPs. All transfections were performed in triplicate. After incubation for 4 h at 37 °C in a 5% CO₂, humidified atmosphere, the medium was aspirated.

Cells were then washed and lysed in order to determine their uptake of NPs. The amount of Pt in cells was measured using ICP-MS.

2.8. In Vitro Drug Release

A suspension of LPI NPs containing 200 µg Pt in 0.1 wt% P85, 50% FBS or PBS was incubated at 37 °C in a shaker at 300 rpm. During different time points, the corresponding samples were centrifuged at 16,000 g for 20 min and the platinum released into the supernatant liquid was measured using ICP-MS.

2.9. Biodistribution

The mice were administered a single dose of 1.0 mg/kg Pt CDDP and LPI NPs. Each group contained five mice, which were sacrificed 4 h following injection. Tissue samples were digested by concentrated nitric acid overnight at room temperature and processed according to the procedure reported previously in the literature. The concentration of Pt was measured using ICP-MS.

2.10. In Vivo Anti-tumor Efficacy Evaluation

Animals were maintained in the Center for Experimental Animals (an AAALAC accredited experimental animal facility) at the University of North Carolina. All procedures involving experimental animals were performed in accordance with the protocols approved by the University of North Carolina Institutional Animal Care and Use Committee and conformed to the Guide for the Care and Use of Laboratory Animals (NIH publication No. 86-23, revised 1985). Female athymic nude mice, 5–6 weeks old and weighing 18–22 g, were supplied by the University of North Carolina animal facility. 1205Lu and A375M xenograft tumors were developed through subcutaneous injection of approximately 5 million tumor cells. Two mg/kg and 1.0 mg/kg of Pt were administered weekly by intravenous (IV) injection for treatment of 1205Lu and A375M tumor bearing mice respectively. Both, tumor growth and body weight were monitored. Tumor volume was calculated using the following formula: $TV = (L \times W^2)/2$, with W being smaller than L . Finally, mice were sacrificed by CO₂ asphyxiation. Tumors were collected after treatment, fixed with formalin and processed for terminal deoxynucleotidyl transferase dUTP nick end labeling (TUNEL) assay.

2.11. TUNEL Assay

Tumors were fixed in 4.0% paraformaldehyde (PFA), paraffin-embedded and sectioned at the UNC Lineberger Comprehensive Cancer Center Animal Histopathology Facility. To detect apoptotic cells in tumor tissues, a TUNEL assay, using a DeadEnd™ Fluorometric TUNEL System (Promega, Madison, WI), was performed, following the manufacturer's protocol. Cell nuclei, which were stained with green fluorescence, were defined as TUNEL-positive nuclei. TUNEL-positive nuclei were monitored using a fluorescence microscope (Nikon, Tokyo, Japan). The cell nuclei were stained with 4, 6-diamidino-2-phenyl-indole (DAPI) (Vectashield, Vector Laboratories, Inc., Burlingame, CA). To quantify TUNEL-positive cells, green-fluorescence-positive cells were counted in three images taken at 40× magnification.

2.12. Detection of Pt-DNA adducts

The CDDP-DNA adducts were detected using anti-CDDP modified DNA antibodies [CP9/19] (Abcam, Cambridge, MA). The sections were incubated with a 1:250 dilution of anti-CDDP modified DNA antibody [CP9/19] at 4 °C overnight followed by incubation with FITC-labeled goat anti-(rat Ig) antibody (1 : 200, Santa Cruz, CA) for 1 h at room temperature. The sections were also stained by DAPI and covered with a coverslip. The sections were observed using a Nikon light microscope (Nikon Corp., Tokyo, Japan).

2.13. Toxicity and Pathology Studies

For liver and renal function experiments, the levels of aspartate aminotransferase (AST), alanine aminotransferase (ALT), and blood urea nitrogen in the serum (BUN) were measured. Major organs were collected after therapeutic treatment and were formalin fixed and processed for routine H&E staining using standard methods. Images were collected using a Nikon light microscope (Nikon).

2.14. Statistical Analysis

Quantitative data were expressed as mean \pm SEM. The analysis of variance is completed using a one-way ANOVA.

3. RESULTS AND DISCUSSIONS

3.1. Preparation and characterization of LPI NPs

Due to the insolubility of CDDP-I in water and organic solvents, current drug loading methods including remote loading, double emulsion and nanoprecipitation, cannot be used to formulate CDDP-I into NPs. CDDP and its derivatives are inorganic, poorly soluble and usually synthesized by mixing the precursor and leaving group-donating compounds, which both are water-soluble. These properties make CDDP and its derivatives unique to other anti-cancer drugs. Microemulsion methods have been successfully utilized to synthesize inorganic nanoparticles, such as silver chloride and calcium phosphate NPs, using a nanoprecipitation process. Therefore, we hypothesize that NPs containing CDDP-I with a controllable size range can also be synthesized *in-situ* using the microemulsion method. DOPA, known to bind to metal ions such as calcium and platinum, was used to stabilize the CDDP-I precipitate and permitted control over the nanoprecipitates' size. The surfactants Igepal and Triton X-100 were used for a similar purpose [14–16]. Without DOPA, the formation of the cores was not well controlled and large aggregates were formed after demulsification with ethanol. DOPA coated cores are water insoluble but soluble in non-polar solvents, such as hexane, chloroform and tetrahydrofuran. Thus, to disperse CDDP-I cores into water, an outer leaflet layer of 1,2-dioleoyl-3-trimethylammonium-propane (chloride salt) (DOTAP), cholesterol, DSPE-PEG and DSPE-PEG-AA were coated onto the CDDP-I cores to form stable LPI NPs.

Hydrated LPI NPs were purified through centrifugation at 10,000 g for 10 min. Drug loading was approximately 82 ± 3 wt%, which was the highest compared to other platinum drug based formulations, and the yield was approximately $42 \pm 6\%$. The size of LPI NPs was examined by TEM and DLS. Cores were about 30–35 nm in diameter (Fig. 1A). Uranyl

acetate staining of TEM images revealed a diameter of about 40 nm (Fig. 1B), a little smaller than the hydrodynamic diameter (40–45 nm) obtained by dynamic light scattering (Fig. 1C). Here, we revealed a concept of formulating an insoluble drug using a hydrophobic lipid coating. Hydrophobic CDDP-I cores can assemble with an outer leaflet lipid, and possibly also with amphiphilic copolymer, such as PEG-PLGA. This provides the opportunity for CDDP-I to be co-encapsulated alongside other hydrophobic drugs.

3.2. Cell toxicities of LPI NPs in 1205Lu and A375M melanoma cells

Following microemulsion synthesis and nanoparticulate formulation of CDDP-I, we proceeded to evaluate the anti-tumor activity of LPI NPs *in vitro*. CDDP was chosen as a control for comparison due to the insolubility and ineffective suspension of CDDP-I. LPI NPs demonstrated a greater efficacy for the inhibition of 1205Lu cells than CDDP alone and had a comparable toxicity against A375M cells (Fig. 2A). These results suggest that LPI NPs are highly toxic to melanoma cancer cells when appropriately formulated. The potent effects of LPI NPs observed *in vitro* might be attributed to the enhanced uptake of the NPs (Fig. 2B).

3.3. In vitro release of the CDDP-I from LPI NPs

In PBS, 50% of the CDDP-I loaded in LPI NPs was released within approximately 80 hours (Fig. 3). The slow kinetics was most likely attributed to the low aqueous solubility and barrier caused by the lipid membrane. To facilitate the release of platinum from LPI NPs, a surfactant, Pluronic® P85, was used to lyse the lipid bilayer. Even a small amount (0.1 wt%) of P85 reduced the release time to approximately 2.5 h from 80 h. This release profile is very similar to the release of doxorubicin from Doxil®, whose interior phase contains crystalline doxorubicin [17]. To further investigate the release mechanism and mimic physiological conditions, a release experiment was performed in FBS medium containing lipases. The release was accelerated 50% of the CDDP-I released in just 6 h. LPI NPs are relatively stable in PBS and can release CDDP-I in the presence of lipase suggesting that NPs remain intact prior to tumor cell uptake.

Traditional liposomal CDDP formulations, such as STEALTH® formulation loaded with CDDP (SPI-077), are characterized by slow drug release rates, which significantly limit the formulation's efficacy. *In vitro* release experiments indicated a negligible release (<10%) of platinum from SPI-077 liposomes after a one-week incubation in serum [18, 19]. Furthermore, *in vitro* cytotoxicity assays indicated that SPI-077 had reduced cytotoxic activity over CDDP, and *in vivo* experiments failed to indicate any superior anti-tumor activity of the liposomal formulation over A375M tumors. However, CDDP-I formulated in LPI-NPs were able to release 50% of platinum within approximately 6.0 h in the presence of 50% serum, a process which was further accelerated when the lipid bilayer was lysed by Pluronic® P85. Adequate release permitted LPI NPs to show superior activity over free CDDP both *in vitro* and *in vivo* in A375M and 1205Lu melanoma xenograft models as discussed below.

3.4. Biodistribution study

The biodistribution of free CDDP versus LPI NPs in A375M tumor-bearing mice was then evaluated. Twenty-four h post IV injection, the CDDP concentration was measured by ICP-MS. Approximately, 9.5% of the injected dose (ID) per gram of LPI NPs accumulated in tumors; significantly higher than the 1.2% observed with free CDDP (Fig. 4). LPI NPs accumulated in the liver and spleen with a similar biodistribution profile to LPC NPs [11]. These organs are expected to be macrophage rich and sites of nanoparticle clearance. LPI NPs showed comparable accumulation to free CDDP in the kidney, where nephrotoxicity was often observed for CDDP treated mice. LPI NPs showed minimal accumulation in the heart.

3.5. In vivo anti-tumor efficacy of LPI NPs on 1205Lu and A375M xenograft tumor

In vivo IV administered LPI NPs had a greater anti-tumor effect than free CDDP in A375M at 1 mg/kg Pt and inhibited the growth of 1205Lu tumors at 2 mg/kg Pt. Significant weight loss was not observed in treated animals (data not shown). Previously, we have shown that LPC NPs, similar formulation to LPI NPs, exhibited a neighbouring effect in killing A375M tumor [11]. Neighbouring effect may be also true for LPI NPs, which induced significant tumor inhibition in A375M tumor. However, the neighbouring effect was not previously observed in 1205Lu tumor. Differences in the tumor microenvironment may also contribute to the less efficient anticancer efficacy of LPI NPs in 1205Lu tumors.

3.6. Cytotoxic effects of LPI NPs in A375M tumor cells

The cytotoxicity of LPI NPs on A375M tumor cells was determined through terminal deoxynucleotidyl transferase dUTP nick end labeling (TUNEL) and staining for Pt-DNA adducts. The TUNEL assay was used to detect DNA fragmentation occurring during apoptosis. Following LPI NPs administration, 15.8% of A375M tumor cells were apoptotic. To indicate that LPI NPs released CDDP-I to inhibit tumor proliferation through the formation of Pt-DNA adducts, tumor sections were stained with a Pt-DNA adduct-specific antibody and confirmed the formation of CDDP-DNA adducts in treated tumors (Fig. 6B). It was observed that the formation of CDDP-DNA adducts was present in 11.9% of tumor cells. Therefore, LPI NPs successfully released active Pt drugs to induce apoptosis in tumor cells through the formation of Pt-DNA adducts. Furthermore data from the *in vitro* release study indicated that release rate could be greatly enhanced in the presence of a surfactant, e.g. P85, to surpass that of the effect of FBS (Fig. 3). This result suggests that the primary factor limiting faster drug release was the lipid bilayer on the surface of the drug precipitate, and not the solubility of the encapsulated drug. It is conceivable that successful drug release inside tumor cells was facilitated by lysosomal lipases, which act to destroy the lipid bilayer when LPI NPs were endocytosed by tumor cells. The released drug then diffuses to induce apoptosis in neighboring cells.

3.7. Safety evaluation of LPI NPs

Nephrotoxicity, a common pitfall of platinum based drugs, was then evaluated and indicated that LPI NPs reduced toxicity over free CDDP at the same dose (Fig. 7). Kidneys treated with LPI NPs showed similar responses to those treated with PBS and no signs of

nephrotoxicity were observed in mice treated with LPI NPs. However, glomerulosclerosis, tubular cell atrophy, and cystic dilatation of renal tubes were observed in kidneys from mice treated with free CDDP at the same dose. Although kidneys were injured at a low dose of CDDP, BUN assay, which was measured 7 days after the last treatment, indicated injured kidneys recovered after a week, because there was no significant difference in BUN results between kidneys from CDDP treated mice and control group (Fig. 8). Pathologic examination of other major organs in mice that received long-term treatments indicated that mice treated with LPI NPs suffered no organ damage. AST and ALT in mice treated with CDDP and LPI NPs fell within the normal range, indicating no significant liver toxicity (Fig. 8). Although considerable spleen accumulation was observed (Fig. 4), no spleen toxicity was observed (Fig. 7). This finding can likely be attributed to macrophage uptake of LPI NPs in the spleen, which is quite resistant to Pt-induced DNA damage due to its strong repair mechanism [20–22]. Additionally, we have previously shown that macrophages in the liver, i.e. Kupffer cells, were quite resistant to LPC NPs, which also uses a platinum based therapeutic [11].

4. Conclusions

The LPI NPs delivery platform was successful in formulating insoluble iodinated CDDP (CDDP-I) into LPI NPs at a significant drug loading efficiency of 82 wt%. *In vivo* studies showed that LPI NPs had comparable or better anti-tumor activity than free CDDP in two different melanoma xenograft models. LPI NPs exhibited a strong EPR effect and accumulated at 9.5% ID/g in an A375M tumor model and induced significant apoptosis without inducing toxicities. The LPI NPs not only showed activity and safety of CDDP-I, but also provides a promising platform for additional formulations of inorganic drugs that are both water and oil insoluble into nanoparticles for therapeutic regimens. Additionally, this platform can be extended as a paradigm for screening and evaluating the anti-cancer efficacy of inorganic compounds.

Acknowledgments

This work was supported by NIH grants CA151652, CA151455 and CA149363. We thank Steven Glenn Plonk and Andrew Mackenzie Blair for their assistance in manuscript preparation.

References

1. Yao X, Panichpisal K, Kurtzman N, Nugent K. Cisplatin nephrotoxicity: A review. *Am J Med Sci*. 2007; 334:115–124. [PubMed: 17700201]
2. Pabla N, Dong Z. Cisplatin nephrotoxicity: Mechanisms and renoprotective strategies. *Kidney Int*. 2008; 73:994–1007. [PubMed: 18272962]
3. Boulikas T, Vougiouka M. Cisplatin and platinum drugs at the molecular level (review). *Oncol Rep*. 2003; 10:1663–1682. [PubMed: 14534679]
4. Rixe O, Ortuzar W, Alvarez M, Parker R, Reed E, Paull K, et al. Oxaliplatin, tetraplatin, cisplatin, and carboplatin: Spectrum of activity in drug-resistant cell lines and in the cell lines of the national cancer institute's anticancer drug screen panel. *Biochem Pharmacol*. 1996; 52:1855–1865. [PubMed: 8951344]
5. Cleare MJ, Hoeschele J. Antitumor platinum compounds. *Platinum Metals Rev*. 1973; 17:2–13.
6. Grinberg AA, Dobroborskaya AI. Water solubility of isomeric diammineplatinum compounds. *Zh Neorg Khim*. 1967; 12:276–277.

7. Aryal S, Hu C-MJ, Zhang L. Polymer-cisplatin conjugate nanoparticles for acid-responsive drug delivery. *ACS Nano*. 2009; 4:251–258. [PubMed: 20039697]
8. Boulikas T. Clinical overview on lipoplatin: A successful liposomal formulation of cisplatin. *Expert Opin Investig Drugs*. 2009; 18:1197–1218.
9. Fonseca C, Simoes S, Gaspar R. Paclitaxel-loaded plga nanoparticles: Preparation, physicochemical characterization and in vitro anti-tumoral activity. *J Control Release*. 2002; 83:273–286. [PubMed: 12363453]
10. Sharma A, Mayhew E, Bolcsak L, Cavanaugh C, Harmon P, Janoff A, et al. Activity of paclitaxel liposome formulations against human ovarian tumor xenografts. *Int J Cancer*. 1997; 71:103–107. [PubMed: 9096672]
11. Guo S, Wang Y, Miao L, Xu Z, Lin CM, Zhang Y, et al. Lipid-coated cisplatin nanoparticles induce neighboring effect and exhibit enhanced anticancer efficacy. *ACS Nano*. 2013; 7:9896–9904. [PubMed: 24083505]
12. Guo S, Miao L, Wang Y, Huang L. Unmodified drug used as a material to construct nanoparticles: Delivery of cisplatin for enhanced anti-cancer therapy. *J Control Release*. 2014; 174:137–142. [PubMed: 24280262]
13. Banerjee R, Tyagi P, Li S, Huang L. Anisamide-targeted stealth liposomes: A potent carrier for targeting doxorubicin to human prostate cancer cells. *Int J Cancer*. 2004; 112:693–700. [PubMed: 15382053]
14. Chiu D, Zhou W, Kitayaporn S, Schwartz DT, Murali-Krishna K, Kavanagh TJ, et al. Biomimetic mineralization and size control of stable calcium phosphate core-protein shell nanoparticles: Potential for vaccine applications. *Bioconjug Chem*. 2012; 23:610–617. [PubMed: 22263898]
15. Velinova MJ, Staffhorst RW, Mulder WJ, Dries AS, Jansen BA, de Kruijff B, et al. Preparation and stability of lipid-coated nanocapsules of cisplatin: Anionic phospholipid specificity. *Biochim Biophys Acta Biomembr*. 2004; 1663:135–142.
16. Burger KN, Staffhorst RW, de Vijlder HC, Velinova MJ, Bomans PH, Frederik PM, et al. Nanocapsules: Lipid-coated aggregates of cisplatin with high cytotoxicity. *Nat Med*. 2002; 8:81–84. [PubMed: 11786911]
17. Zhao Y, Alakhova DY, Kim JO, Bronich TK, Kabanov AV. A simple way to enhance doxil(r) therapy: Drug release from liposomes at the tumor site by amphiphilic block copolymer. *J Control Release*. 2013; 168:61–69. [PubMed: 23474033]
18. Barenholz Y. Doxil(r)--the first fda-approved nano-drug: Lessons learned. *J Control Release*. 2012; 160:117–134. [PubMed: 22484195]
19. Bandak S, Goren D, Horowitz A, Tzemach D, Gabizon A. Pharmacological studies of cisplatin encapsulated in long-circulating liposomes in mouse tumor models. *Anticancer Drug*. 1999; 10:911–920.
20. Li X, Wang LK, Wang LW, Han XQ, Yang F, Gong ZJ. Cisplatin protects against acute liver failure by inhibiting nuclear hmgb1 release. *Int J Mol Sci*. 2013; 14:11224–11237. [PubMed: 23712360]
21. Basu A, Krishnamurthy S. Cellular responses to cisplatin-induced DNA damage. *J Nucleic Acids*. 2010; 2010
22. Kang TH, Lindsey-Boltz LA, Reardon JT, Sancar A. Circadian control of xpa and excision repair of cisplatin-DNA damage by cryptochrome and herc2 ubiquitin ligase. *Proc Natl Acad Sci USA*. 2010; 107:4890–4895. [PubMed: 20304803]

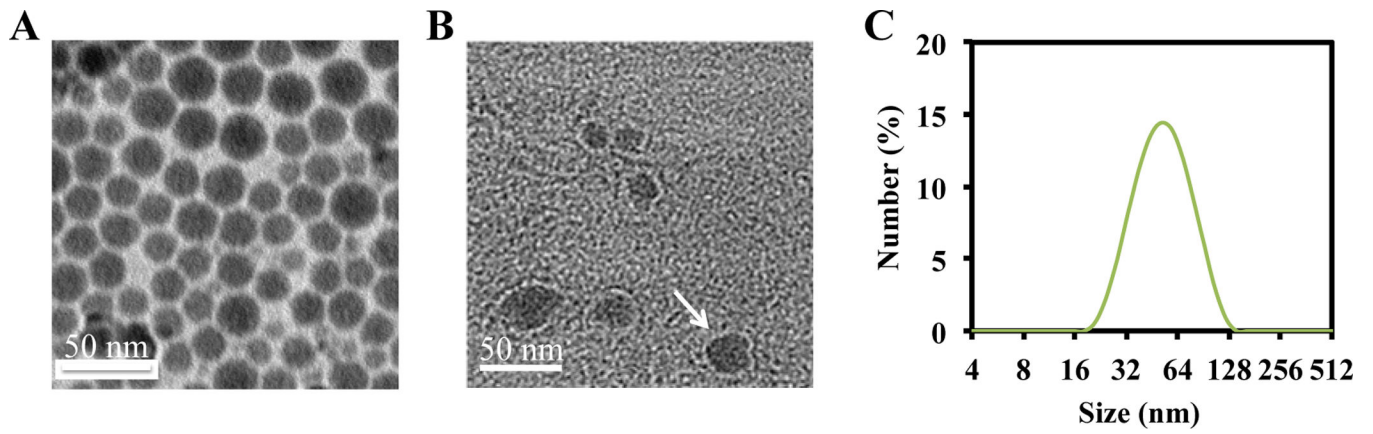


Fig. 1. Characterization of CDDP-I cores by TEM (A) and characterization of LPI NPs by TEM (B) and DLS (C). LPI NPs were negatively stained using uranyl acetate. White arrow indicates bilayer of LPI NPs.

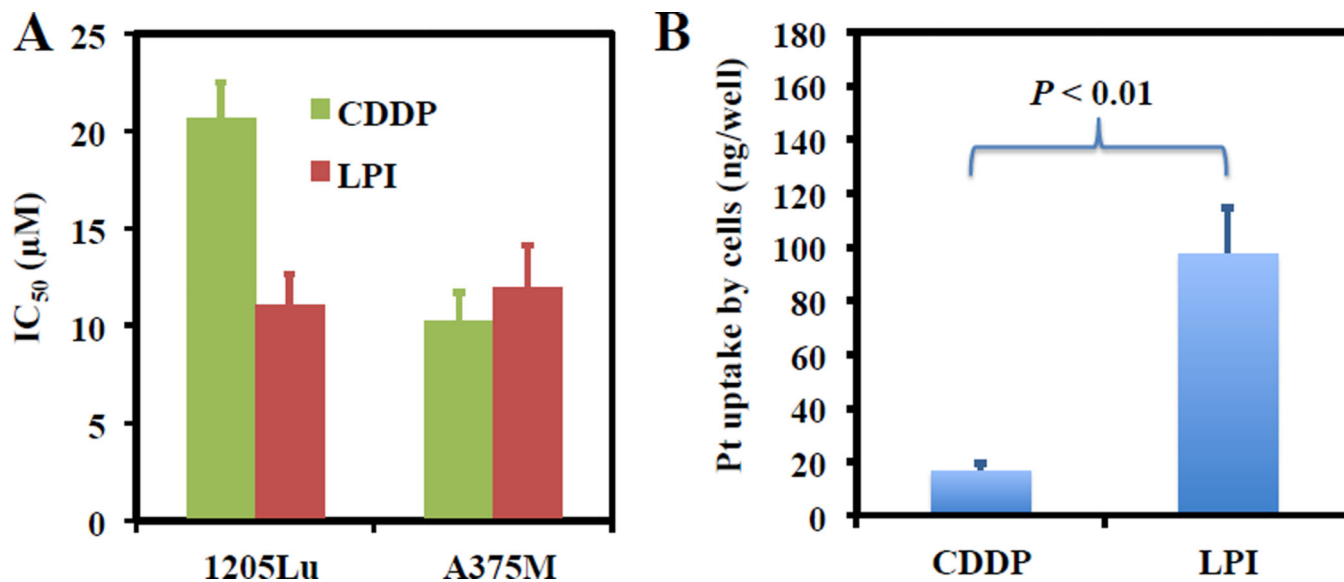


Fig. 2.

IC₅₀ values of LPI NPs in 1205Lu and A375M cells (A). The amount of the Pt drug associated with A375M cells after incubation with 100 µM CDDP or LPI NPs in 24 well plates (B). Each bar represents the mean ± SEM of 3 independent experiments. The analysis of variance is completed using a one-way ANOVA.

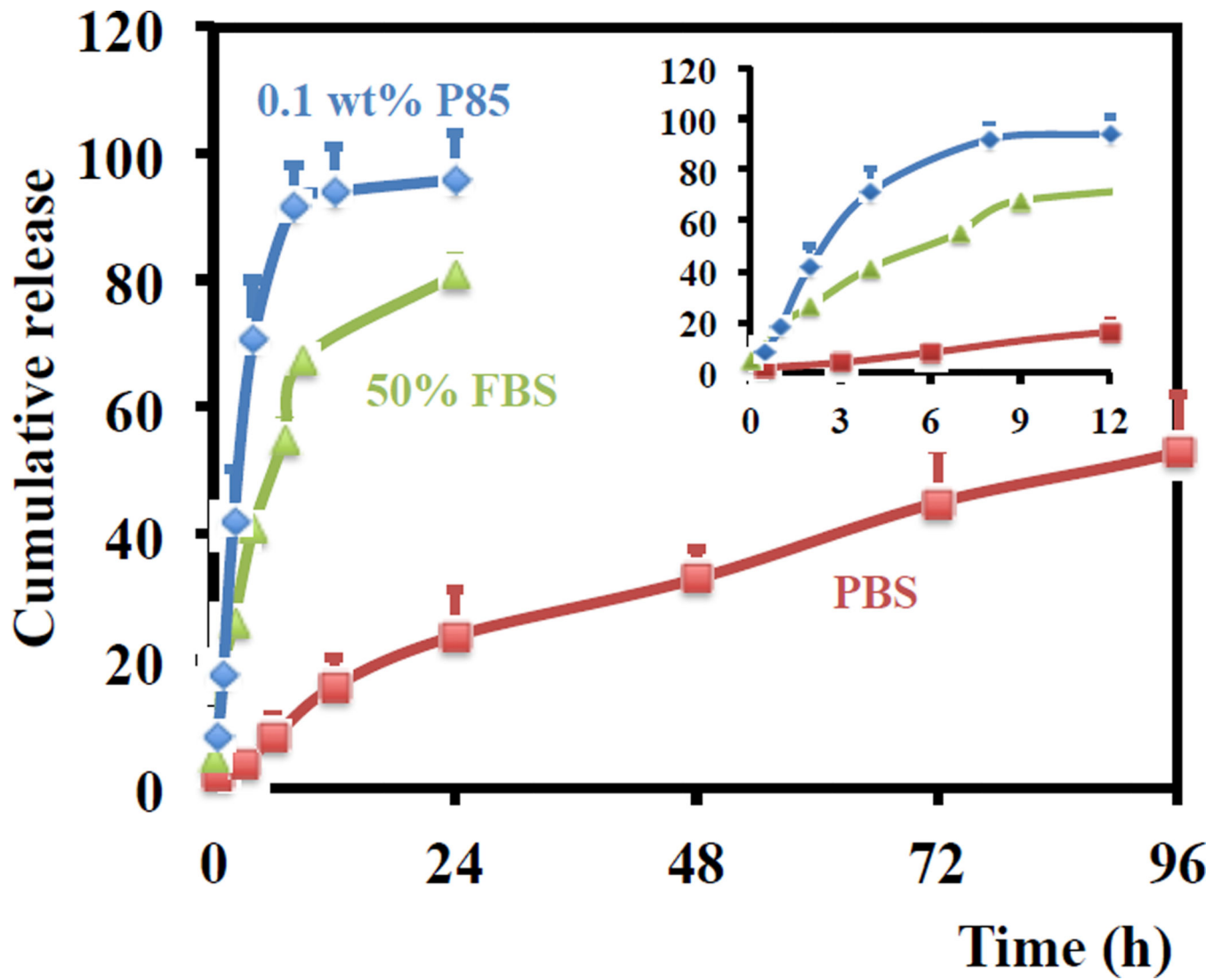


Fig. 3.
In vitro release of platinum from LPI NPs in 0.1 wt% P85, 50% FBS and PBS at 37 °C.
Data are expressed as mean \pm SD (n = 3).

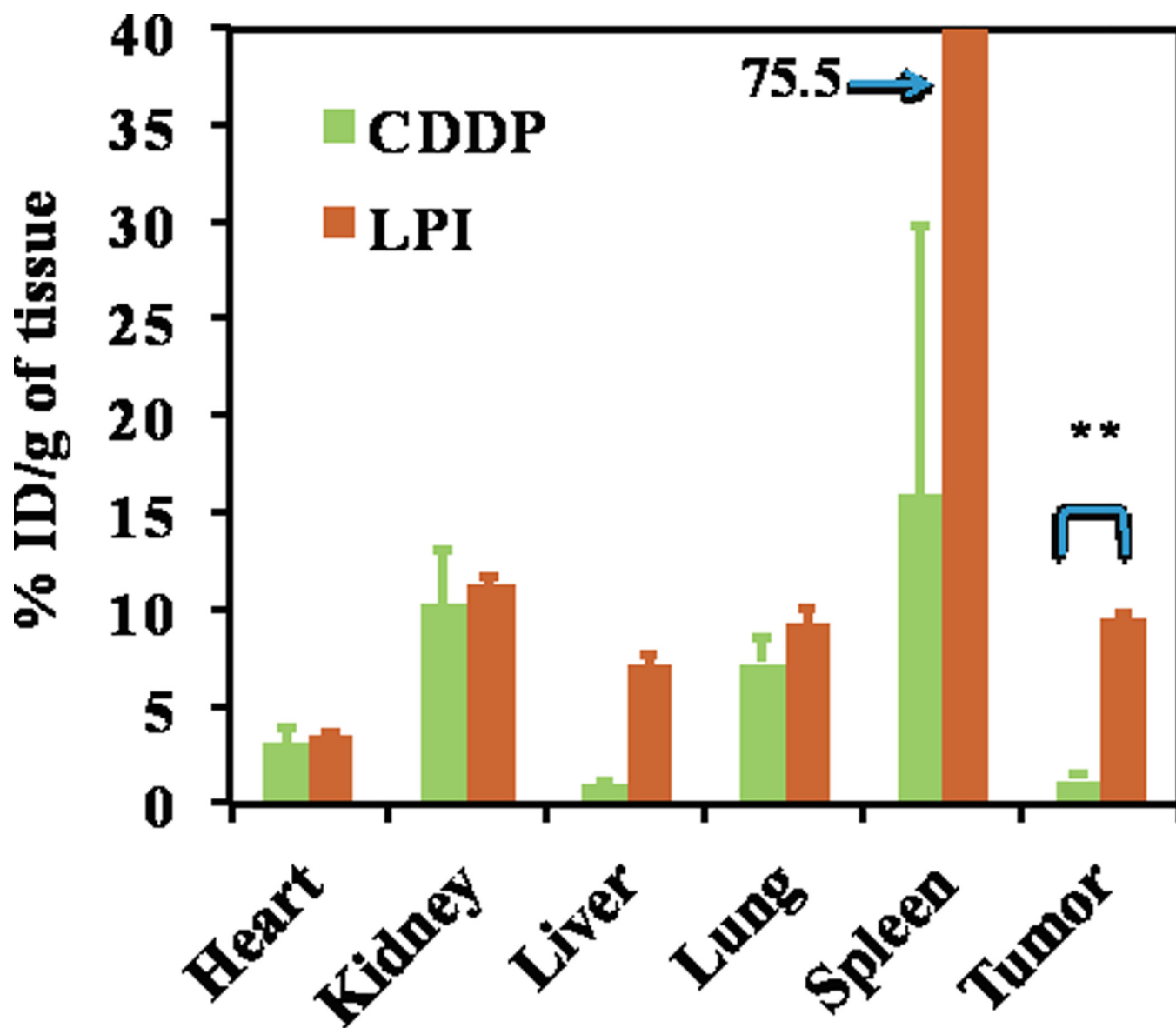


Fig. 4. Pt distribution in A375M tumor bearing mice administered with CDDP and LPI NPs. One mg/kg of Pt was administered through IV injection. Mice were sacrificed 24 h post IV injection. The results are displayed as mean \pm SEM (error bars) of five animals per group. The analysis of variance is computed using a one-way ANOVA. ** indicates $P < 0.01$.

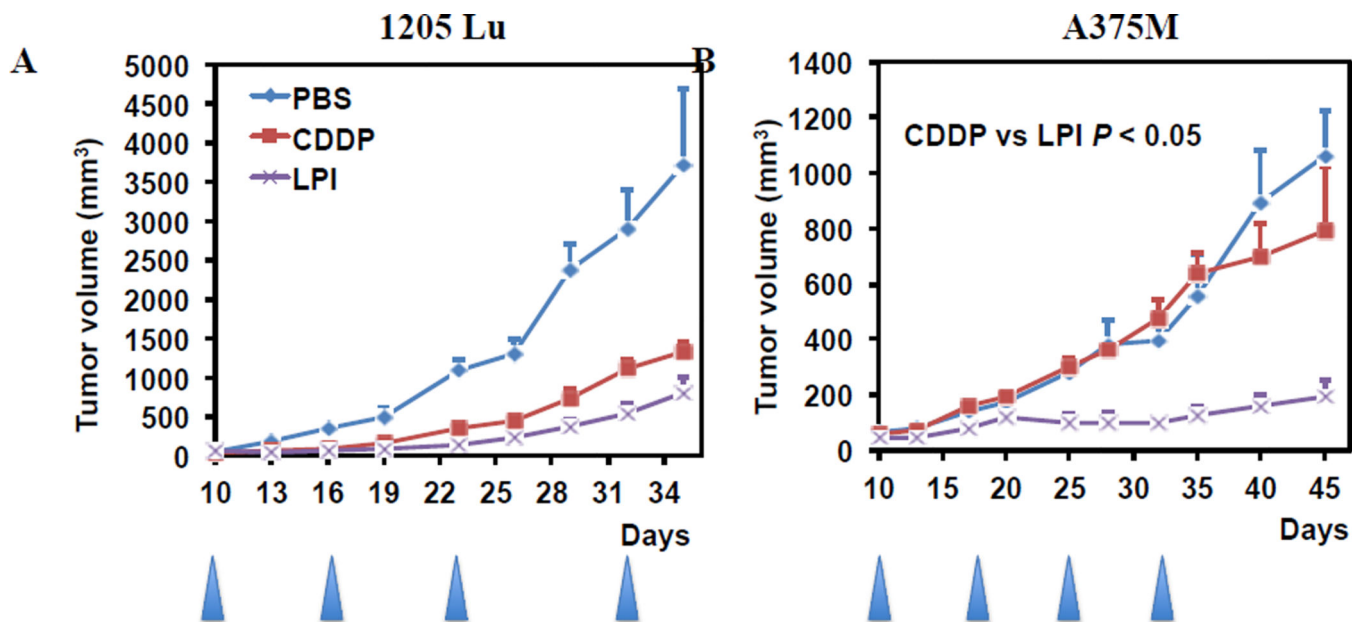


Fig. 5. The effect of CDDP and LPI NPs on growth of 1205Lu (A) and A375M (B) tumors *in vivo*. The arrowheads indicate the time of injection. Two and one mg/kg of Pt was administered weekly *via* IV injection for 1205Lu and A375M tumor bearing mice respectively. The results are displayed as mean \pm SEM (error bars) of five animals per group. The analysis of variance was computed using a one-way ANOVA.

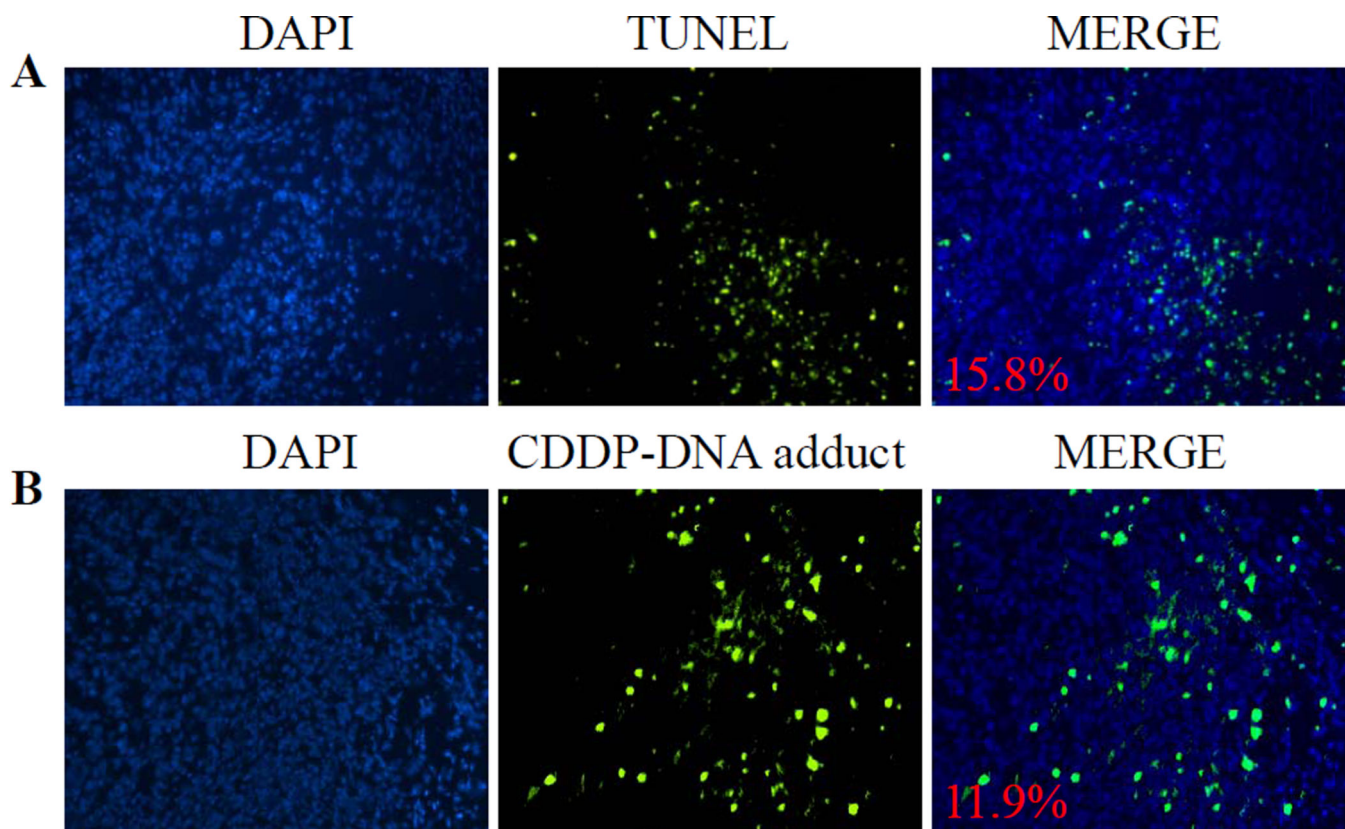


Fig. 6. TUNEL assay and detection of CDDP-DNA adduct in an A375M tumor model. The mice were sacrificed 24 h after receiving a single IV injection of LPI NPs at a dose of 1.0 mg/kg Pt. The apoptotic tumor cells were detected by the TUNEL assay (A, green); the formation of CDDP-DNA adducts in tumor cells were detected by CDDP-DNA adduct antibody (B, green). Cell nuclei were stained with DAPI. The number represents the percentage of apoptotic cells (A) or CDDP-DNA adduct positive cells (B).

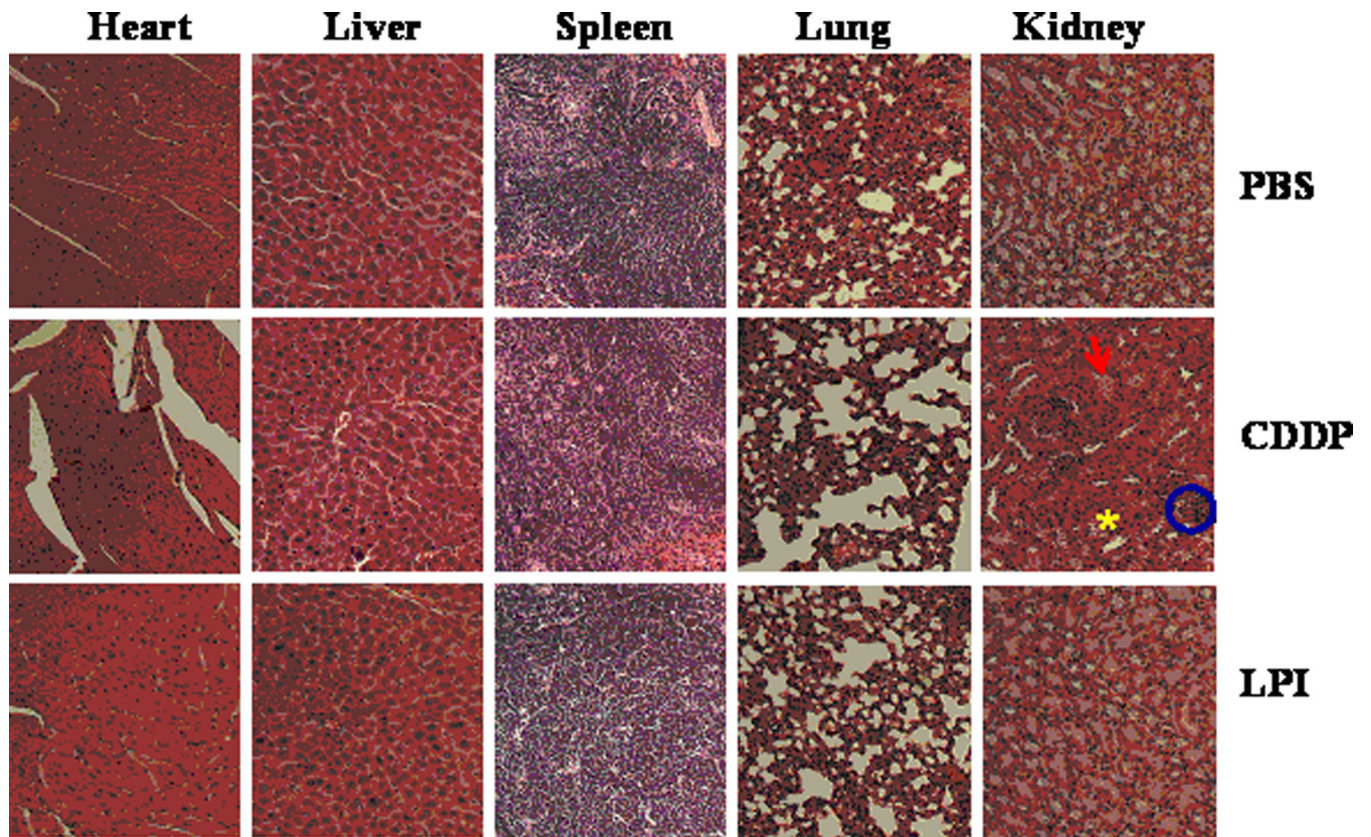


Fig. 7. H&E staining of heart, liver, spleen, lung and kidney tissue from mice that received four doses of treatment (1 mg/kg each). H&E staining showed LPI NPs did not induce nephrotoxicity. Circles indicated glomerulosclerosis; arrows indicated tubular cell atrophy; asterisk indicated cystic dilatation of renal tubes.

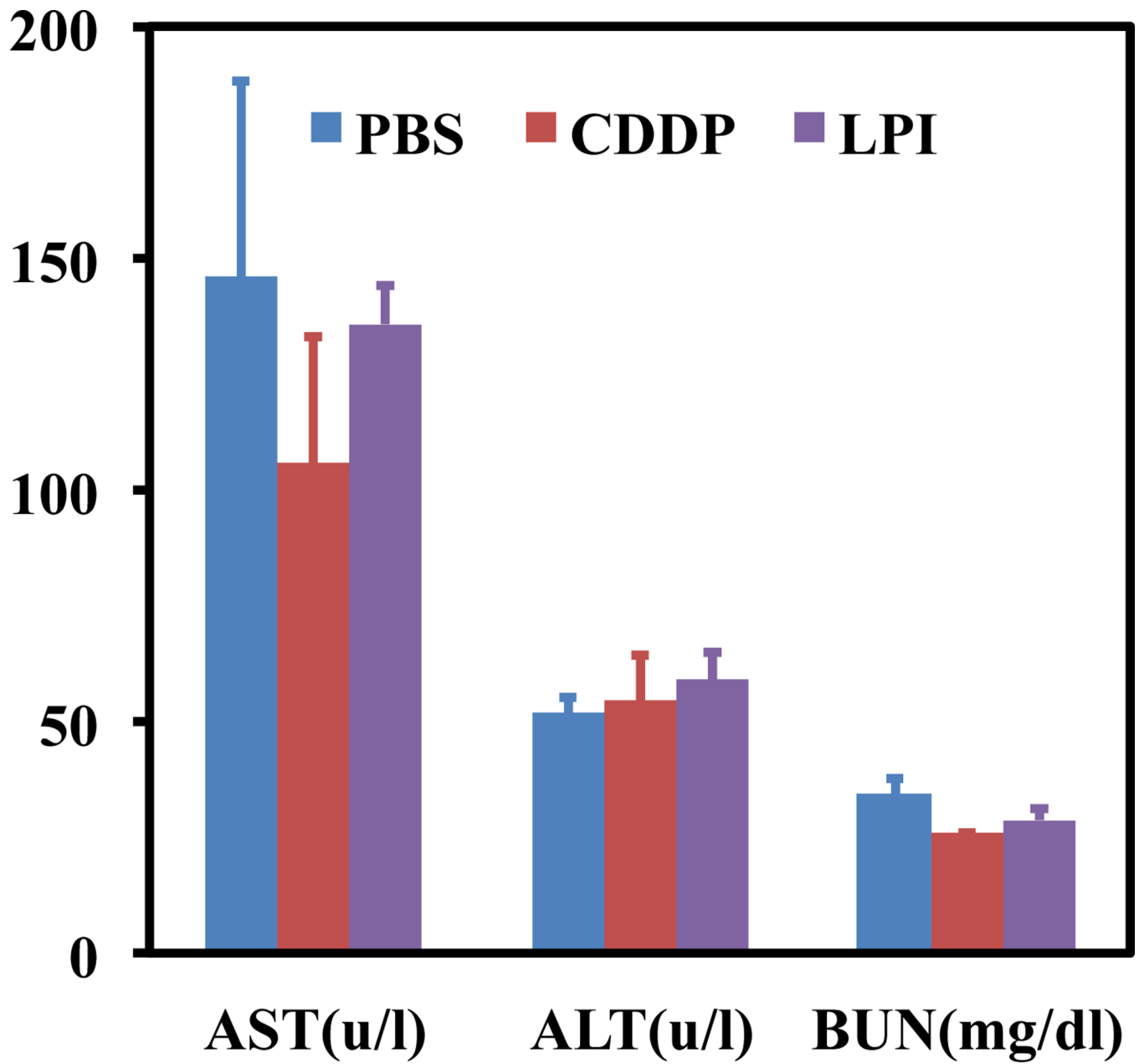
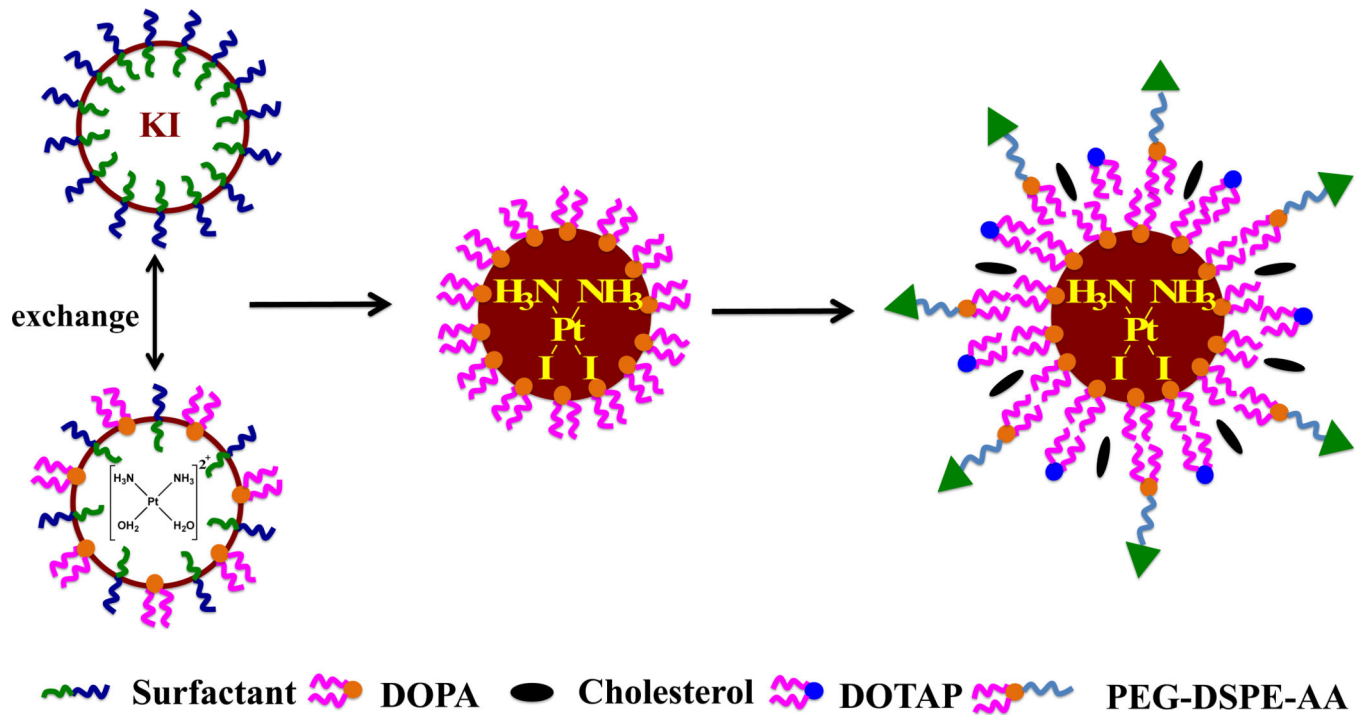


Fig. 8. Liver and kidney functional parameters, AST (aspartate aminotransferase), ALT (alanine aminotransferase) and BUN (blood urea nitrogen).



Scheme 1.
Synthesis of LPI NPs and structure of iodinated cisplatin (CDDP-I).